Case Studies in Construction Materials 16 (2022) e00932

Contents lists available at ScienceDirect

Case Studies in Construction Materials

journal homepage: www.elsevier.com/locate/cscm

Effectiveness of carbon textile reinforced concrete in shear strengthening short-span corroded reinforced concrete beams

Dang Quang Ngo, Huy Cuong Nguyen *, Huu Tai Dinh, Duy Tien Nguyen, Dinh Loc Mai

University of Transport and Communications, No.3 Cau Giay street, Hanoi, Viet Nam

ARTICLE INFO

Keywords:
Shear strengthening
Corrosion
Textile-reinforced concrete
Repeated load

ABSTRACT

This paper will present the shear behavior of the corroded stirrups reinforced concrete (RC) beams strengthened with textile reinforced concrete (TRC). The shear resistance contributions from the corroded RC beams and carbon TRC at various volume ratios were carefully examined. Eighteen beams were tested, including twelve subjected by an electrochemically accelerated aging technique for 60 and 90 days to obtain the theoretical mass loss in their stirrups of 10% and 20%, respectively. The stirrups were locally corroded in the shear span. After the corrosion accelerating treatment, corrosion cracks on concrete surfaces were marked, and their widths were measured to observe their distributions. A three-point bending test was applied to obtain the shear performances of the corroded beams subjected to the monotonic and repeated loading. Eight corroded RC beams were strengthened using 2 and 3 U-wrap layers of bidirectional carbon textile. The shear behavior will be discussed, including the ultimate capacity, failure mode, load-deflection, load–strain relationship, and crack distributions. Compared to the controlled specimens, the averaged shear strength of corroded specimens decreased by 16.08% and 25.34%, corresponding to the degree of corrosion ranging from 12.3% to 23.6%. The experimental results also demonstrate that the shear capacities of the corroded RC beams strengthened with carbon TRC had been improved 60.6% compared to the severely corroded controlled specimens.

1. Introduction

Deficiencies in existing RC structures may become serious due to natural ageing, increased required load capacity, deterioration caused by corrosion, and other causes. Corrosion of embedded reinforcing steel is widely accepted as the primary contributor causing premature damage of RC structures, including reducing steel reinforcement area, loss of bond strength, and loss of concrete area, influencing the concrete cover and cross-section. Currently, there are numerous methods available to retrofit RC beams in flexure and shear, each with relative advantages and weaknesses. The most preferable, efficient and practised techniques for shear strengthening are RC jacketing and FRP wrapping [1]. However, using section enlargement with RC to enhance shear capacity, the thickness of the jacket, in typical cases higher than 70–100 mm, leads to the increased total mass of the structure and decreasing esthetics in architecture. This method is also not very suitable for RC structures in corrosive environments. In contrast, FRP wrapping has advantages over concrete jacketing methods such as less thickness, lower weight and better constructability. Even though the technique was used

* Corresponding author.
E-mail addresses: ngodangquang@utc.edu.vn (D.Q. Ngo), nguyenhuycuong@utc.edu.vn (H.C. Nguyen), taidh@utc.edu.vn (H.T. Dinh), ngduytien@utc.edu.vn (D.T. Nguyen), maidinhloc@utc.edu.vn (D.L. Mai).

https://doi.org/10.1016/j.cscm.2022.e00932
Received 21 October 2021; Received in revised form 25 January 2022; Accepted 6 February 2022
Available online 7 February 2022

widely, it also has some durability limitations due to the weakness of the epoxy resin. The drawbacks such as low heat tolerance, lack of fire resistance, degradation under ultraviolet light, and poor compatibility with the concrete surface could not be overcome.

Textile reinforced concrete is an emerging repair method in which multi-axial high strength textile reinforcements are applied to the structure's surface using fine-grained concrete. With the advent of TRC, a new strengthening approach has come to the fore used in degrading buildings in harsh environments. The technology was also introduced as the fiber-reinforced cementitious matrix (FRCM) in America [2]; textile-reinforced mortar (TRM) in Europe. TRC shares some of the advantageous properties of FRP and has overcome some of its limitations. A valuable feature of TRC is its excellent resistance to high temperatures, fire exposure, and UV radiation. Besides, TRC has good compatibility with the concrete substrate [3], leading to easier monitoring of the concrete cracks developed after strengthening. TRC systems can be operated in dual functional capacities [4], including structural strengthening and electro-chemical corrosion protection for corroded RC structures via the impressed current cathodic protection method [5].

In literature, in the field of application of TRC, extensive research was done in strengthening non-corroded RC beams [6–19], while a few focused on corroded ones [20–23]. Previous studies examined in strengthening non-corroded RC beams have mainly investigated the flexural and shear behaviors through experimental, finite element and analytical approaches (e.g., Brückner et al. [3], Wiberg et al. [7], Babaeidarabad et al. [8], D'Ambrisi et al. [9], Hussein et al. [10], Sneed et al. [11]). All of these studies reported that the application of TRC could considerably increase in ultimate capacity of strengthened structures. The critical parameters analyzed in these studies were the percentages of textile reinforcement (expressed by the number of layers), steel reinforcement ratio, material properties, and strengthening configuration. For shear strengthening, Escrig et al. [17] studied the performance of beams strengthened by different textile materials, including basalt, carbon, PBO, and glass. It was concluded that the bond between matrix-textile and the bond between TRC-concrete substrate significantly affects the TRC system's performance. Tetta et al. [18] reported that using U-wrapped configuration will guarantee a better performance of the strengthened beam than the side bonded one. Blänksvard et al. [14] strengthened RC beams using TRC made of different mortars and carbon textile types. Blanksvärd concluded that using fine-grained concrete with higher mechanical properties and fibers could improve TRC systems' performance. Contamine et al. [16] tested two average TRC thicknesses in strengthening damaged RC beams and concluded that the thickness of reinforcement did not significantly affect the strength gains of the strengthened specimens.

Up to the present, only a few works have studied the flexural performance of TRC-strengthened corroded RC beams [20–23]. Besides, no studies were found on corroded RC beams upgraded in shear with the TRC. Elghazy et al. [20] used CFRP, carbon-TRC, and polyparaphenylene benzobisoxazole (PBO)-TRC to strengthen corroded RC beams. He found that both carbon- and PBO- TRC would effectively rehabilitate the original flexural strength of the uncorroded beam. Furthermore, the PBO-TRC-strengthened specimen showed higher performances than those of CFRP and carbon-TRC-strengthened specimens in terms of strength. El-Maaddawy et al. [21] studied the flexural behavior of corroded T-beams, upgraded with carbon and basalt-TRC material. It was reported that the basalt-TRC could not retrieve the original flexural capacity of the uncorroded beam, whereas the carbon-TRC regenerated 109% of the capacity. Oluwadahunsi et al. [23] used TRC for flexural strengthening of corroded TRC beams, with the mass losses of the tension steel at midspan approximately 10% and 20%. Within this work, the ultimate capacity of corroded beams increased from 5.3% to 26%. The U-shape configuration also provided the best performance in terms of load–deflection response and energy absorption recovery. Liang Fang et al. [22] compared the flexural performance of corroded RC slabs strengthened with basalt-TRC and basalt-FRP. The results also showed that the strengthening effects of basalt-FRP and basalt-TRC were affected by the initial corrosion ratio and the number of textile layers. In an intermediate state of corrosion (8%), the flexural capacities and deflection capacities of RC slabs strengthened by BFRP and BTRC were increased substantially; the flexural capabilities were increased by 27.81–61.85%.

2. Research significance

Clearly, corrosion of the steel reinforcements is one of the main causes of deterioration of TRC beams. Corrosion of stirrups is often more severe than longitudinal bars, leading to possible shear failure, which will occurred in a brittle manner. Even though most corroded RC members exhibit a reduction in shear capacity in practice, studies on the effectiveness of TRC jacketing in shear strengthening of such members are still lacking. Many RC structures such as bridges or parking garages endure repeated loading from vehicles, which causes substantial deterioration of bond strength between reinforcing bars and concrete as well as stress concentration at rebars, especially when they are corroded.

This paper presents the performances of corroded short-span RC beams strengthened externally with carbon TRC. The corroded beams were subjected first to repeated loading and then to monotonic, both under three-point bending test. Performance of strengthened members under repeated loading plays a vital role for the method to be considered for structures with variable loads, such as bridges. The test parameters include corrosion levels, strengthening layers, load types (monotonic or repeated load), and load range applied. A corrosion accelerating process has been implemented in research to achieve the desired mass loss in a timely manner. This study contributes to understanding the effect of new strengthening technique on the behavior of corroded RC beams.

3. Experimental investigation

3.1. Test program

This study focused on retrofitting RC beams that contained corroded stirrups, considering an extreme case of corrosion. The steel stirrups in RC beams were assumed to be moderate and severely corroded, resulting in moderate and severe losses in steel cross-section and bond strength. Carbon TRC was used to strengthen the deteriorated RC beams. Eighteen RC beams were classified into three main

Table 1
Test beams description.

Group	Name	Load type	Description
G1: Un Corroded	R0-1, R0-2	Static	No stirrup
	R1-1, R1-2	Static	Reference beams to obtain the shear strength in static loading (P_{max})
	R2-1, R2-2	Repeated	Un-corroded control RC beam,
G2: Corroded Level 1 (moderate)	L1R1, L1R2	Repeated	Corroded control beam for Group 2
	L1S2-1, L1S2-2	Repeated	Corroded beam + TRC with 2 textile layers
	L1S3-1, L1S3-2	Repeated	Corroded beam + TRC with 3 textile layers
G3: Corroded Level 2 (severe)	L2R1, L2R2	Repeated	Corroded control beam for Group 3
	L2S2-1, L2S2-2	Repeated	Corroded beam + TRC with 2 textile layers
	L2S3-1, L2S3-2	Repeated	Corroded beam + TRC with 3 textile layers

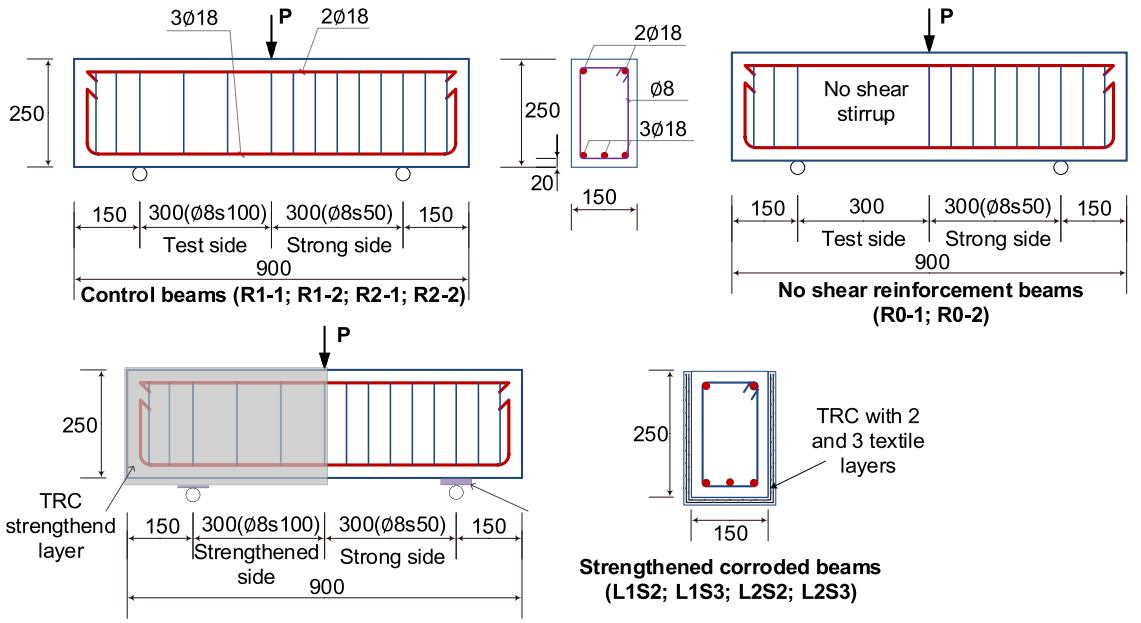

Fig. 1. Details of test specimens.

groups based on the theoretical mass loss of reinforcing bars caused by corrosion. The first group consisted of 6 un-corroded beams, which was tested to compare against corroded and repaired specimens. The second and third groups consisted of six beams facilitated by an accelerated corrosion process to induce specified theoretical mass loss of 10% (moderate level) and 20% (severe level), respectively. These specimens were then wrapped by two or three U-shape layers of carbon TRC. A detailed description of specimens is as follows. The specimens with references initial letter 'R' were un-strengthened beams; specimens with regards initial letter 'S' was TRC-strengthened specimens. The specimens marked with 'L1' or 'L2', which stands for corrosion level 1 or level 2, were targeted to have a mass loss of 10% or 20%, respectively (Table 1).

3.2. Specimens description

This program constructed eighteen RC beams with a rectangular cross-section of 150 × 250 mm. Each beam was 900 mm long and was supported over the clear span of 600 mm, following the three-point bending configuration. The shear span was 300 mm, corresponding to the shear slenderness (shear span to depth) equals 1.36. The RC beams were designed to provide a flexural capacity significantly larger than the shear capacity in unstrengthened form. The stirrups were calculated in such a way that all beams will be directly failed in one half of the beam span (namely, "test side"). Only the "test side" was subjected to an electrochemically accelerated ageing and then strengthened in shear with carbon TRC. The external TRC was provided in the form of U-wraps over the entire shear span (Fig. 1).

Fig. 1 also displays the detailed reinforcement layouts of all beams. In the first group, two beams (namely R0-1 and R0-2) with no shear reinforcement on the test side were used to obtain the concrete contribution to the total shear capacity. All of the remaining beams have the same configuration. The longitudinal deformed reinforcing bars are all 18 mm in diameter. As for compression one, two of them are placed on the top and three for tension on the bottom side of the section. The shear reinforcement was identical in all cases (except for beam R0-1 and R0-2) and consisted of 8 mm diameter stirrups. The steel shear reinforcement on the two sides was

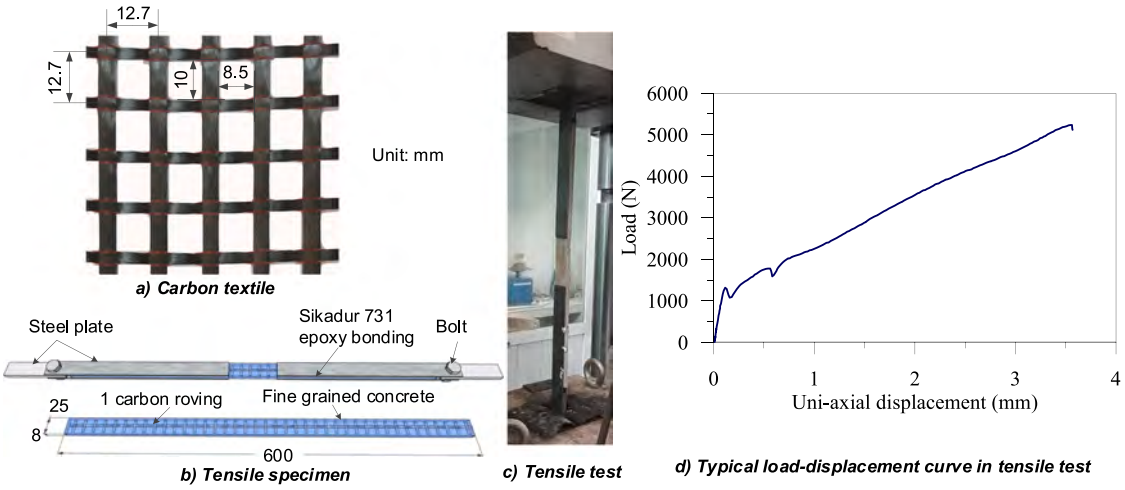

Fig. 2. Carbon textile and TRC specimen for the uniaxial tensile test.

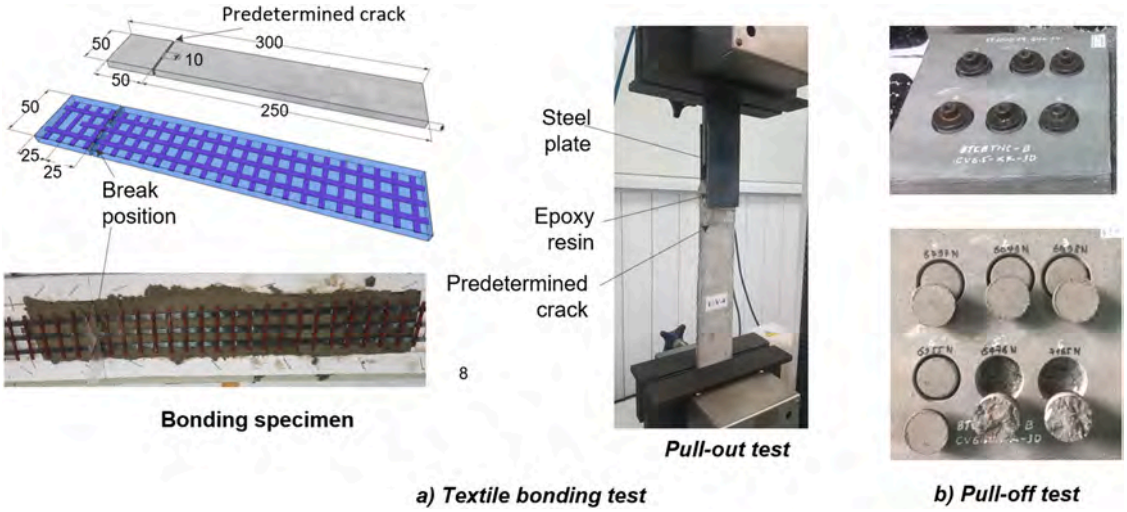

Fig. 3. Pull-out test and pull-off test.

designed to ensure failure on the "test side", while the other half was over-reinforced (strong side). The stirrups with a distance of 100 mm were reinforced in the "test side". On the contrary, the shear reinforcement consists of 10 steel bars with a spacing of 50 mm in the heavily reinforced shear span ("strong side").

3.3. Materials specification

All specimens were fabricated using concrete with an averaged compressive strength of 38.5 MPa measured with the cylinder at 28 days. Because the spacing between the stirrups is relatively small, the coarse aggregate selected was pea gravel, having a nominal maximum size of 10 mm. The longitudinal reinforcing bars and stirrups' actual yield strengths were 429.4 MPa and 363.1 MPa, respectively.

The TRC strengthening layer proposed for this program consists of carbon textile fabric and fine-grained concrete. The maximum aggregate size is only 0.63 millimeters to provide a suitable bonding property with textile rovings. It has also consisted of high-quality cement, fly ash, and a superplasticizer. The compressive strength and flexural tensile strength of fine-grained concrete were 45.2 MPa and 5.3 MPa, respectively.

An orthogonal textile SITgrid017 made of intersecting carbon fiber was used as shear reinforcement (Fig. 2). The carbon textile has an orthogonal grid size of 12.7 mm, surface weight 578 g/m^2, and 50–50% weight distribution in the two directions. Each roving consists of 48.000 fibers, corresponding to the fineness of 3200 tex, and the cross-sectional area of 1.808 mm^2. The filaments were are coated with styrene-butadiene during fabrication. The measured tensile strength of the rovings was 2890 MPa, which was obtained from the uni-directional tensile test (Fig. 2), following the Recommendation of RILEM TC 232-TDT [25]. The elastic modulus was

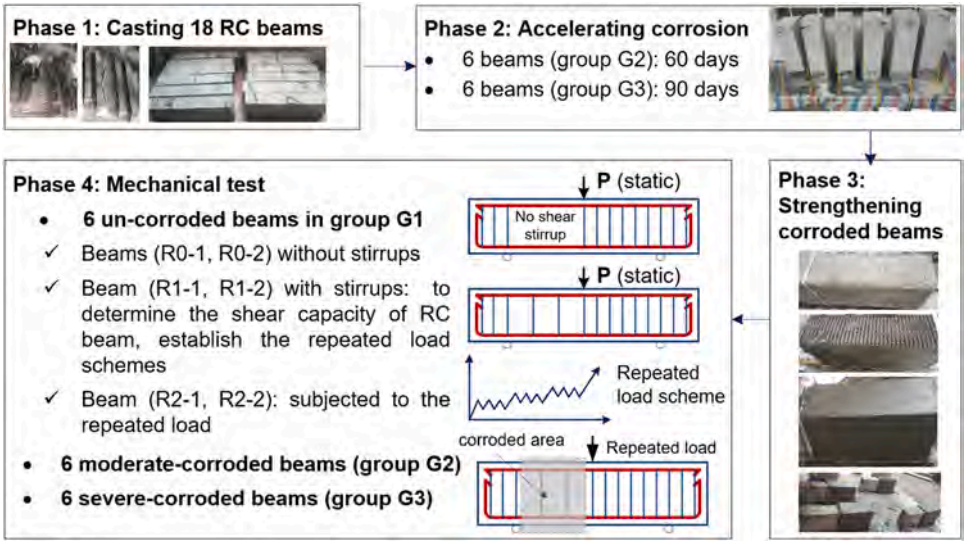

Fig. 4. Experimental program.

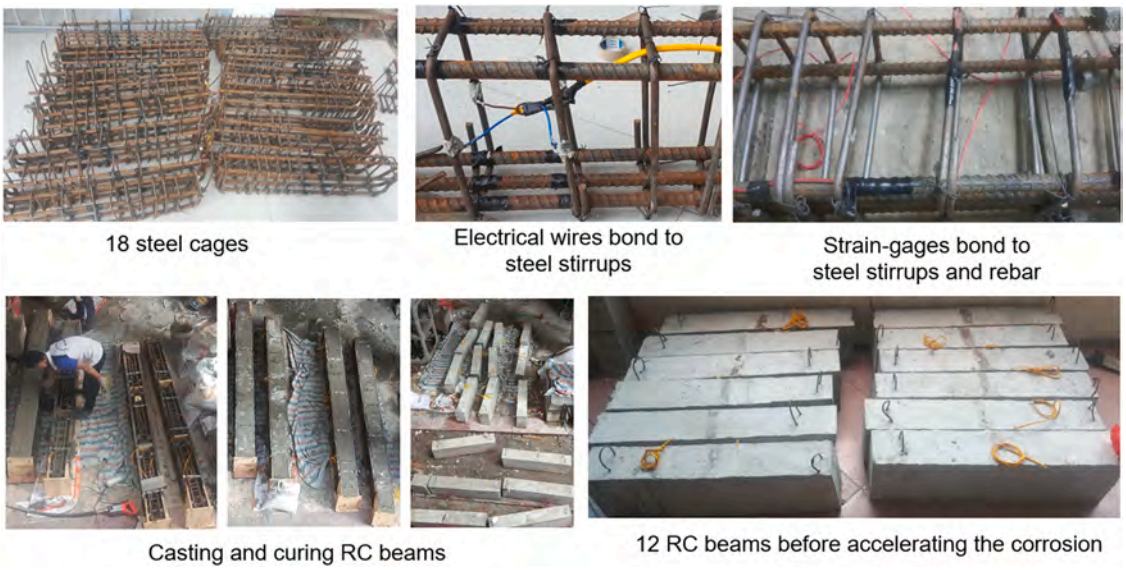

Fig. 5. Casting RC beams procedures.

determined at about 185 GPa.

The bond behavior between textile reinforcement and surrounding concrete matrix was performed by the pull-out test recommended by German Guide Zulassung Z-31.10-182 [26]. In the pull-out experiment, a TRC specimen with a 300 mm × 50 mm × 8 mm dimension was were prepared (Fig. 3-a). A PE sheet was placed at the beginning of the bond length in the specimens to initiate the first crack, which occurs at the predetermined breaking point. Thus, a roving with an embedding length of 25 mm was pulled out gradually from the fine-grained concrete. The average bonding strength (force per length) was found to be 18.8 N/mm.

The interfacial behavior was studied through a pull-off test in which a fine-grained concrete layer is applied onto the substrate, following the general procedures of the AC434 guideline [24]. A 50 mm diameter circular cut was made on the fine-grained concrete layer and into the concrete substrate. A steel plate was attached to the fine-grained concrete surface, and then the pull-off test was performed (Fig. 3-b). The primary failure mode has occurred at the concrete/overlay interface. The pull-off strength, which was computed based on the maximum indicated load, was approximately 3.7 MPa.

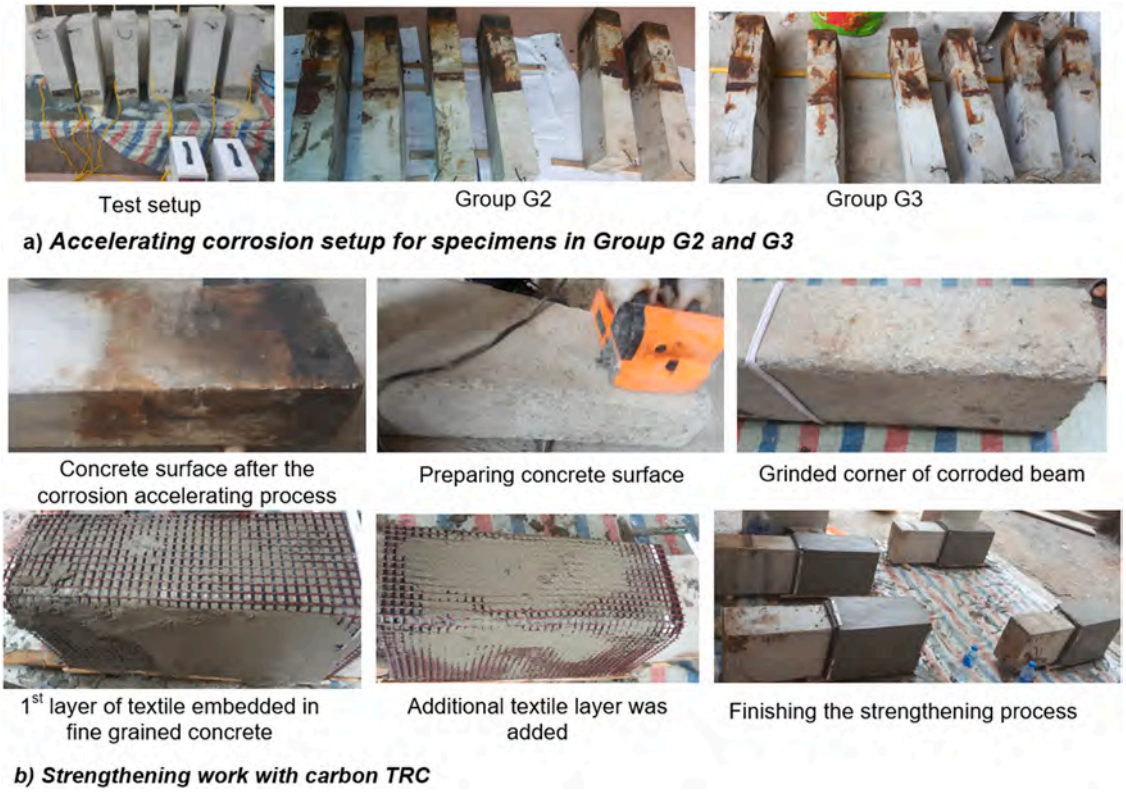

Fig. 6. Accelerating corrosion setup and strengthening work.

3.4. Test procedures and instrumentation

The experimental procedure consisted of four major phases (Fig. 4). Phase one included preparing the beam specimens from forming to the end of the curing process. Phase two was the accelerated corrosion process. This consisted of the circuit setup and the steps taken to monitor the progression of the samples while they were undergoing corrosion. Phase three was the strengthening work to upgrade corroded specimens with U-shaped jackets of TRC. Phase four was the mechanical testing phase of the research process. All specimens were tested in identical setups to compare results effectively. Phase four also included the demolition of beams and collecting data of the corroded stirrups after the experiment.

3.4.1. Phase 1: casting RC beams

In this study, corrosion was controlled to occur only in the "test side" region, from the load-to-support span. The reinforcing cage was assembled outside and then inserted in the formwork after the strain gauges and electrical wires were glued to the assigned individual rebar and stirrups (Fig. 5). Corrosion in the steel stirrups was accelerated using an electrochemical method. Two hoops served as the anode and were subjected to an electrical current from the DC power supply. The contact surfaces between stirrups and rebars were separated by electrical tape. All 18 beams were cast at a time. After fabrication of the forms and assembly of the steel cage, the concrete was mixed and poured. The concrete surface was then covered with wetted burlap and plastic sheets.

3.4.2. Phase 2: reinforcement corrosion acceleration process

To achieve the corroded theoretical levels within a short time, the corrosion process of the reinforcing steel was accelerated. The corrosion acceleration technique was applied to corrode the stirrup by imposing an electrical current on the reinforcement. As mentioned earlier, 18 beams were cast, including six beams left un-corroded to serve as reference beams, and 12 beams underwent the corrosion process. In this process, 12 specimens, making up two groups of 6 beams, were continuously placed in the tank. Fig. 6-a illustrates the schematic representation of the setup. The tank was filled with an electrolytic solution with 5% sodium chloride (NaCl) by water weight. These beams were placed standing vertically up to a depth of 450 mm or half of the beam's length. The beams were connected in series; the stirrups and the copper plates would be the anode and the cathode. The electrolyte solution was changed every two weeks to keep the constant value of NaCl concentration. The voltage was recorded daily as part of the accelerated corrosion monitoring in this study. In addition, every week, the beams were lifted from their tanks to observe cracking and measure crack's width propagation due to corrosion.

Based on Faraday's law, the current density was chosen approximately 400 $\mu A/cm^2$, while the time required to reach the desired

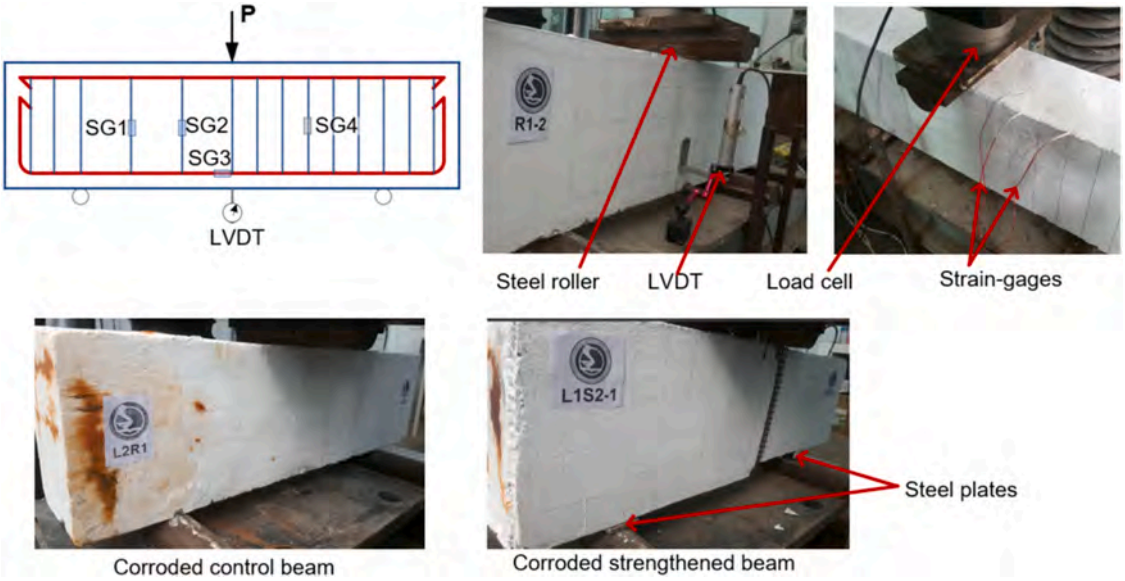

Fig. 7. Test setup and instrumentations.

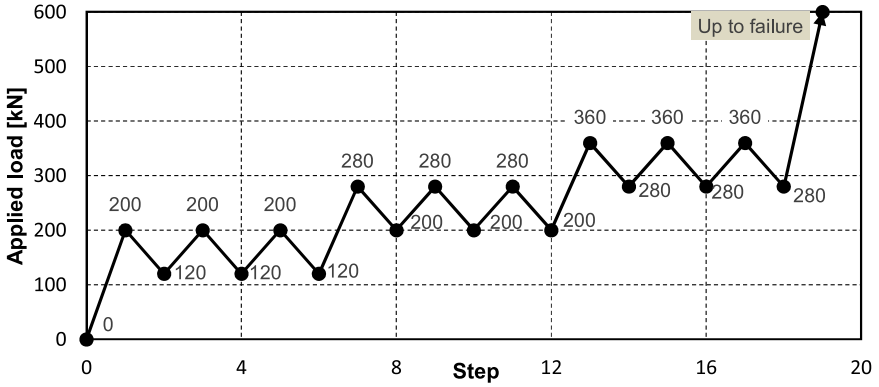

Fig. 8. Repeated load scheme.

corrosion levels was calculated 60 days and 90 days. It should be noted that Faraday's law was under-predicted at a lower corrosion rate and over-predicted at a higher corrosion rate [26]. Thus, the calculated time to reach the theoretical mass loss was increased by 30% to account for the under prediction.

3.4.3. Phase 3: strengthening works

After completing the corrosion process, four beams in each group were wrapped with two and three textile layers, and the rest stayed unstrengthened as for references. The TRC strengthening layer was applied following a procedure mentioned in ACI 549.4R-13 [1]. Substrate preparation, including removal of corrosion dust improvement of surface roughness, was conducted to provide an excellent interfacial bonding between TRC and concrete substrate. A concrete planer machine was employed to remove the weak layer from the beam's surface and grind the beam's corners (Fig. 6-b).

All the strengthened beams were strengthened partly in the form of U-jackets for the "test span" only. Using a metal trowel, the first layer of fine-grained concrete was applied to the surfaces of the corroded beam first with a thickness of 4 mm. The textile was then pressed slightly into the fine-grained concrete to embed the textile layer in the concrete matrix. The second concrete layer was added to cover the textile fabric entirely with 3–4 mm thickness. The procedure was repeated until reaching the designed number of textile layers.

3.4.4. Phase 4: mechanical tests

All tests were performed in a Universal Testing Machine by forced control, and the loading rate was set to be 0.5 kN/s. To measure the mid-span deflections, an LVDT was attached to the bottom surface of the beams. Four strain gages (SG1–SG4) were installed to record the tensile strain of the longitudinal rebars and shear stirrups. To avoid the stress concentration problems, three steel plates

Table 2
Summary of tested results.

Group	Beam	Actual mass loss (%)	Ultimate load (kN)
G1:Un-Corroded	R0-1	NA	220.6
	R0-2		226.2
	R1-1		395.6
	R1-2		384.3
	R2-1		398.6
	R2-2		429.5
G2: Corroded Level 1 (moderate)	L1R1	12.3	353.4
	L1R2	14.7	340.7
	L1S2-1	12.8	476.5
	L1S2-2	13.6	467.0
	L1S3-1	12.5	498.4
	L1S3-2	11.9	524.1
G3: Corroded Level 2 (severe)	L2R1	23.6	313.5
	L2R2	21.9	304.0
	L2S2-1	19.8	449.2
	L2S2-2	21.7	430.6
	L2S3-1	23.3	501.5
	L2S3-2	22.9	490.2

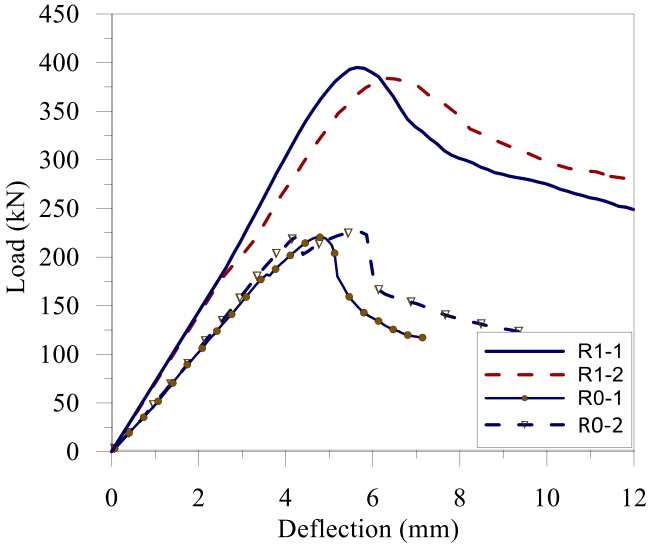

Fig. 9. Load-deflection of four uncorroded specimens subjected to monotonic load.

embedded inside concrete beams were used. The arrangement for the beams testing with LVDTs and strain gage locations is also presented in Fig. 7.

The first four beams in Group G1 were loaded monotonically up to failure to evaluate the ultimate capacities, which was used to create the load ranges used in the repeated tests. The remaining 14 beams were firstly tested under repeated loading and then loaded statically until failure (Fig. 8). The load ranges were determined by the ultimate load P_{max} of specimens R1-1 and R1-2 (the ultimate load P_{max} was then determined approximately 400 kN). Three load ranges, including (0.3–0.5) P_{max}, (0.5–0.7) P_{max}, and (0.7–0.9) P_{max}, were chosen, with three cycles for each range. These load ranges were selected to demonstrate service load, low overload, and high overload levels.

4. Results and discussion

4.1. The behavior of un-corroded specimens (Group G1)

The primary result data obtained from the test are summarized in Table 2. Fig. 9 and Fig. 11 show the behavior of 6 un-corroded control specimens concerning applied loads and deflections. The formation of cracks in the series is displayed in Fig. 10. As expected, failure of six un-corroded beams was in shear; no bending failure occurred. During the test, some limited vertical cracks were observed, but dominant cracks, caused by shear, developed diagonally from the support to the point of applied loads. A critical large shear crack forming from the support to the point of applied loads controlled the failure behavior of the tested beams in this group.

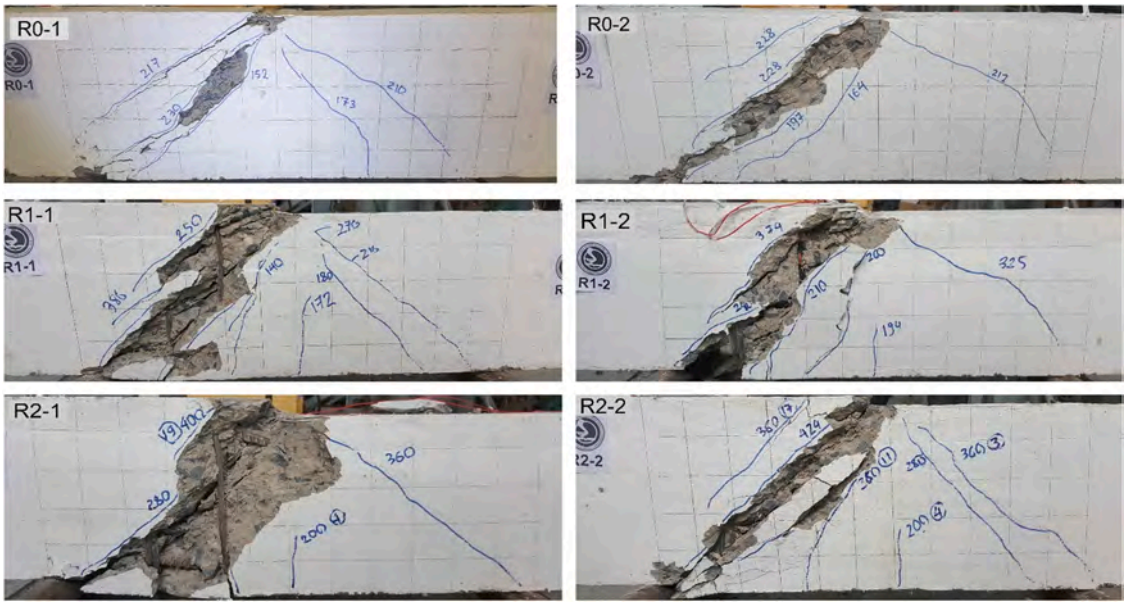

Fig. 10. Crack patterns of six uncorroded-control specimens.

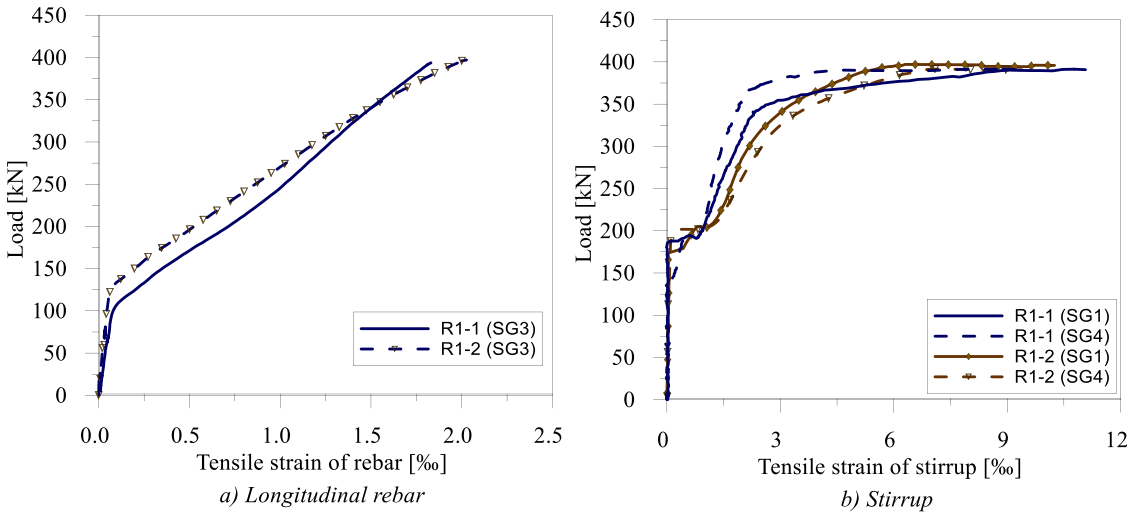

Fig. 11. Load-strain relationships of specimens R1-1 and R1-2.

At first, two control specimens, R0-1 and R02, with no shear reinforcement in the "test side", were monotonically tested. These behaved as expected, failed in shear with the large diagonal cracks. The crack development was similar for both beams. The first diagonal crack started to appear in a load range of 152–164 kN. Then, some more cracks formed and propagated diagonally towards the corners of the applied load (Fig. 10). After reaching the ultimate load (at a load level around 222 kN), the diagonal cracks extended, and the beam failed suddenly without warning signs.

In the second static-load test applied on un-corroded specimens (R1-1 and R1-2), the first visual bending cracks appeared at the midspan at the load levels of 172 kN and 194 kN. These flexural cracks extended further upward to the applied load position as the load increased. The initiation and propagation of shear cracks can be seen around 180 kN and 210 kN for beams R1-1 and R1-2, respectively (Fig. 10). After this point, shear cracks became more extensive and developed towards the supports and the loading points. In the absence of shear links in specimen R1-1, the crack initiated at the "test side" showed a much steeper angle than in specimen R0-1, which did not provide stirrups. As can be seen from the load-deflection relationship, the shear reinforcement intends to increase the stiffness of the beams R1-1 and R1-2 compared to the beams R0-1 and R0-2 (Fig. 9). The initial stiffness of beams R1-1 and R1-2 was almost linear elastic, and the loss in stiffness was observed after the pronounced shear cracks.

As expected, these beams failed at the "test side/weak side". The shear strengths of tested beams R1-1 and R1-2 recorded during the

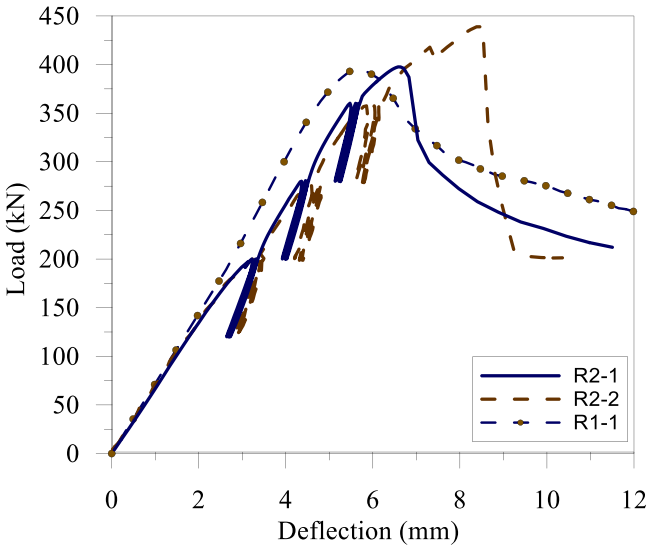

Fig. 12. Shear behavior of R2-1 and R2-2 under the repeated load.

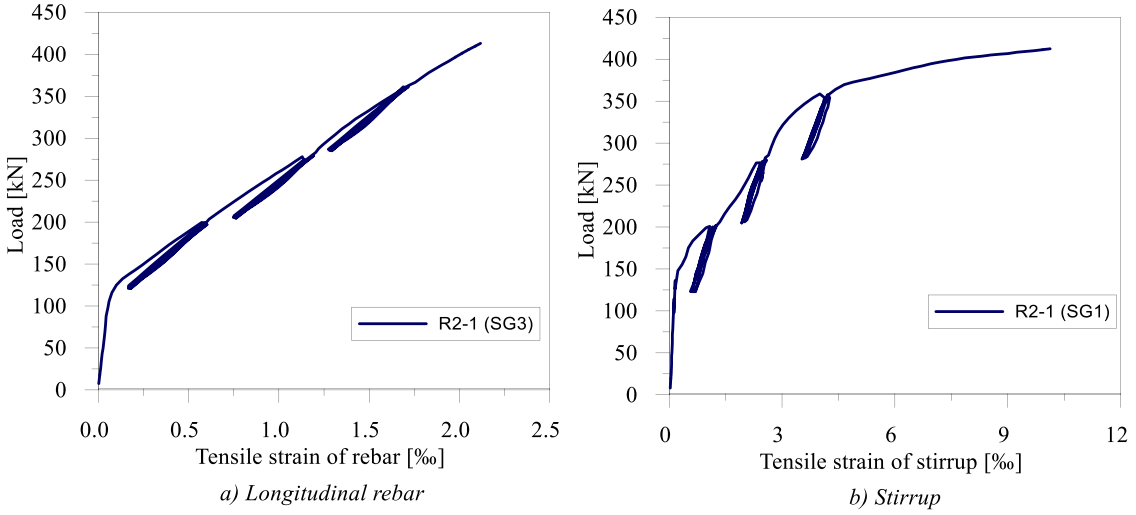

Fig. 13. Load-strain relationships of beam R2-1 under repeated load.

shear tests are 398.6 kN and 384.3 kN, respectively. The percent increase in the ultimate strength of the specimens reinforced by the stirrups compared to un-reinforced specimens was 74.5%. The steel stirrups in the short-span beams assisted in carrying a portion of applied shear forces. Further applying the shear loads, the shear cracks occurred extensively along the shear spans of tested beams, and the tested beam failed gradually. The first four beams in Group G1 were monotonically loaded, while the other two beams (R2-1 and R2-2) were subjected to the repeated load. The repeated load ranges were determined by the maximum load P_{max} of the specimens R1-1 and R1-2, approximately 400 kN (Fig. 9).

The readings from strain gauges installed in longitudinal bars and stirrups are displayed in Fig. 11. Fig. 11-b showed that the stirrup's strains of beam R1-1, R1-2 far exceed the limit of yielding strain, which is approximately 0.002 in steel stirrups. However, once concrete cracking occurred at around 125 kN, the tensile strain in rebar at the midspan started to increase steadily as expected. The strains were about 0.0018 when shear failure took place in specimens R1-1 and R1-2, which means the rebar has not yielded yet.

In specimens R2-1 and R2-2, the first visual flexural cracks started around 200 kN at a midspan deflection of 3.2 mm. Then, the other flexural cracks were inclined to develop shear cracks at the load range of 200–280 kN due to the combination of shear force and bending moment. The diagonal shear cracks started to occur at the applied loads of 280 kN (at the "test side") and 360 kN (at the "strong side"). After shear cracks appeared, the load increased with the smaller stiffness due to the aggregate interlocking effect and the longitudinal rebars' dowel action (Fig. 12). However, these beams displayed a smaller stiffness than specimen R1-1 (subjected to static load). The more fine flexural-shear cracks started to develop approximately from the midpoint of the shear span and extended to the

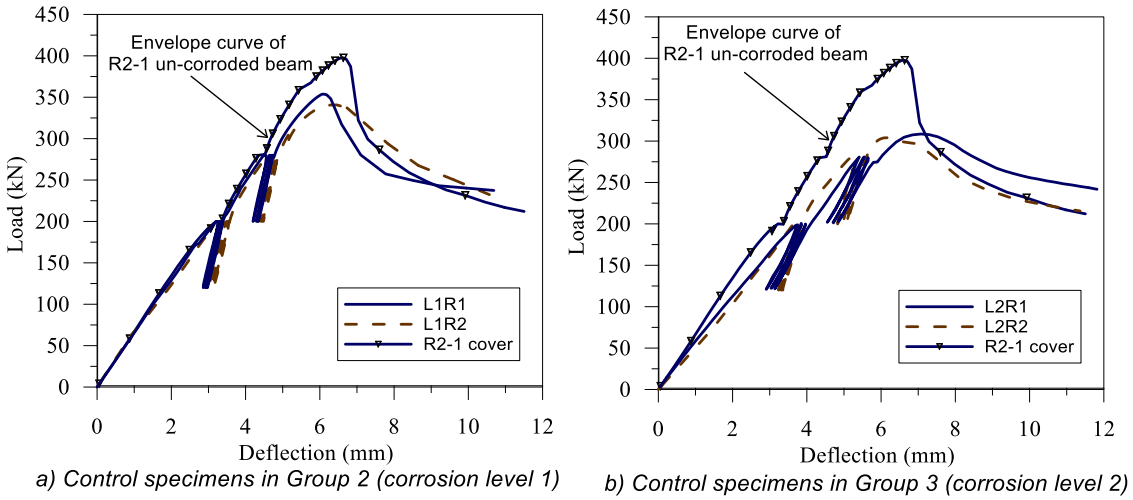

Fig. 14. Shear performances of corroded-unstrengthened specimens.

point of load application with increased loading, as shown in Fig. 10. While the flexural cracks observed were narrower, the diagonal cracks spread more expansive than the un-repeated beams. The load-deflection curves after cyclic loading are almost linear up to the peak. The failure occurred due to the large diagonal shear crack extension at the average load level of 409 kN. The measured strains of transverse and longitudinal bars in beam R2-1 are drawn in Fig. 13. Similar to beam R1-1, the strains stirrups at failure far exceed the yielding strain of its steel. Once yielding occurred at 240 kN, the strain in the stirrup kept increasing. The maximum strains observed in the long longitudinal rebar were smaller than the yielding strain of the rebar's steel.

4.2. The behavior of corroded – unstrengthened specimens

The experimentally obtained load-deflection relationships of the corroded-unstrengthened beams in the 2nd and 3rd groups were displayed in Fig. 14. After finishing the repeated load tests, the beams were demolished, and the stirrups were recovered for visual examination and evaluation of the weight loss resulting from the corrosion process (Fig. 15 and Fig. 18). The first flexural cracks occurred at around 165 kN and 182 kN in the corroded beams L1R1 and L1R2, respectively. By increasing the applied load, the cracks started to incline. Due to the effects of corrosion on stirrups, the first shear cracking loads was much smaller than those in the un-corroded specimens. The first shear crack was observed in specimens L1R1 and L1R2 at the load level of 214 kN and 226 kN. The stiffness of the corroded beams L1R1 and L1 R2 of Group 2 was not much affected by corrosion despite the reduction in shear resistance. Both specimens were failed in shear at the load levels of 353.4 kN and 340.7 kN, which were not completed in the high overload range of (0.7–0.9) P_{max}. Compared to the controlled specimens (R2-1 and R2-2), the shear strength of specimens L1R1 and L1R2 decreased by 14.5% and 17.6%, respectively.

At the end of the tests, the corrosion rates were calculated from weight loss measurements. The resulting corrosion rates ranged from 11.9% to 23.6% for the shear stirrups in the 2nd and 3rd groups (Table 2). The actual mass loss results were slightly higher than the calculation following Faraday's law. The corrosion damages in specimens L1R1 and L1R2 were generally distributed along with the whole stirrups. However, the localized pitting corrosion significantly caused the section loss in specimens L2R1 and L2R2.

All four corroded-unstrengthened beams in Group G2 and Group G3 exhibited similar load-deflection behavior, with the large shear cracks having a dominant development compared with flexural cracks. However, the specimens L2R1 and L2R2 displayed a slightly reduced stiffness relative to the un-corroded beams. This was more evident at the higher degrees of stirrups corrosion, and the severe corrosion led to a decrease in stiffness and thus an increase in deflection. The pitting corrosion can be seen in the extracted steel stirrup of RC beams in Group 3 (more severe corrosion). The shear strengths of beams L2R1 and L2R2 recorded during the repeated tests are 313.5 kN and 304.0 2 kN. The pitting corrosion has essential effects on the degradation of RC beams, with a severe reduction of up to 25.3% in the ultimate strength compared to control beams.

4.3. The behavior of corroded–strengthened specimens

The crack distributions of the corroded-strengthened specimens were displayed in Fig. 15 and Fig. 18. In general, the failure is attributed to the large inclined cracks and rupture of fibers in strengthened specimens with two-carbon layers. The failure of the three-carbon layers strengthening specimens began by crushing concrete struts in RC beams' "strong side". Fig. 16 and Fig. 17 display the load venus deflection curves of the controlled and the strengthened specimens. In general, the U-wrapped TRC layer helped enhance the stiffness and load-bearing capacity of the corroded RC beams.

The flexural cracks developed first for the TRC-strengthening specimens in Group 2 (moderate corrosion). Due to the section enlargement with TRC, the initial stiffness of strengthened beams was also higher than that of control beams. As the load increased,

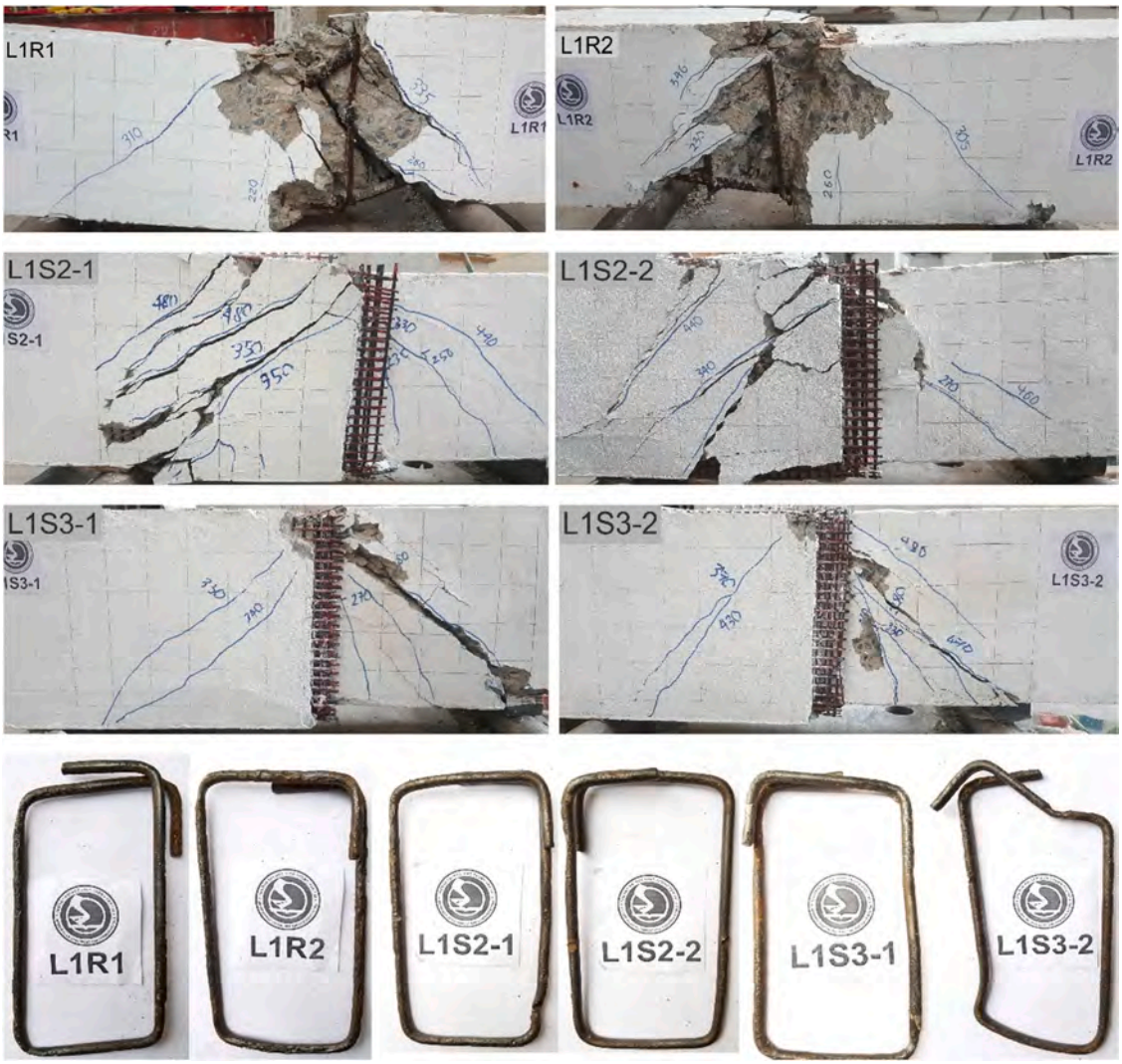

Fig. 15. Crack patterns of corroded specimens in Group 2 and the extracted-corroded stirrups.

these flexural shear cracks started to form. It is important to note that the shear cracks occurred at loads much higher than those in the control beams and changed from the test side to the strong side. The first shear cracks were observed in Specimens L1S2-1, L1S2-2, L1S3-1, and L1S3-2 at the load of 240 kN, 210 kN, 270, and 255 kN. Compared between Specimens L1S2-1 and L1S3-1, an increasing number of textile layers led to an increase of first shear crack load. In specimens L1S2-1 and L1S2-2, the ultimate failure was due to the rupture of textile rovings in the U-wrapped layers, followed by the large inclined cracks at the "test side". Compared to the corroded-controlled specimens (L1R1 and L1R2), the ultimate load of beams L1S2-1 and L1S2-2 increased by 37.3% and 34.6%, respectively. The deflection at failure was 7.9 mm, slightly more than that of corroded-controlled beams. The remaining load in the strengthened beams was much higher than that of the control beams due to the existence of pull-out textile rovings. At the diagonal crack, the transverse rovings with long bond length failed by the tensile rupture, while short bond length rovings failed by complete pull-out. These pull-out textile rovings could carry a small tensile load due to the friction between the roving and fine-grained concrete.

Similarly, strengthening by three U-wraps textile layers in specimens L1S3-1 and L1S3-2 provide 43.6% and 51.0% increases in shear bearing capacity compared to the non-strengthened corroded specimens. Due to the more considerable amount of textile reinforcement and fine-grained concrete, the repaired beams displayed an increased stiffness than the un-strengthened beams. Moreover, a large shear crack developed a shear span at the strong side and extended up to a point close to the load application point, while smaller flexural-shear cracks were displayed on the strengthened side. However, the beams did not fail in the "test side" like 2-layers-strengthened beams since a large amount of external shear reinforcement prevented it. Both strengthened beams failed by concrete crushing on the strong side (un-corroded span), while the tensile break of textile reinforcement did not occur.

As the shear reinforcement experienced extremely corrosive (ranged from 19.8% to 23.3%) in Group G3, the flexural shear cracks started to form at smaller load levels than those in Group G2. As displayed in Fig. 17 and Table 2, the TRC layer also helped enhance the

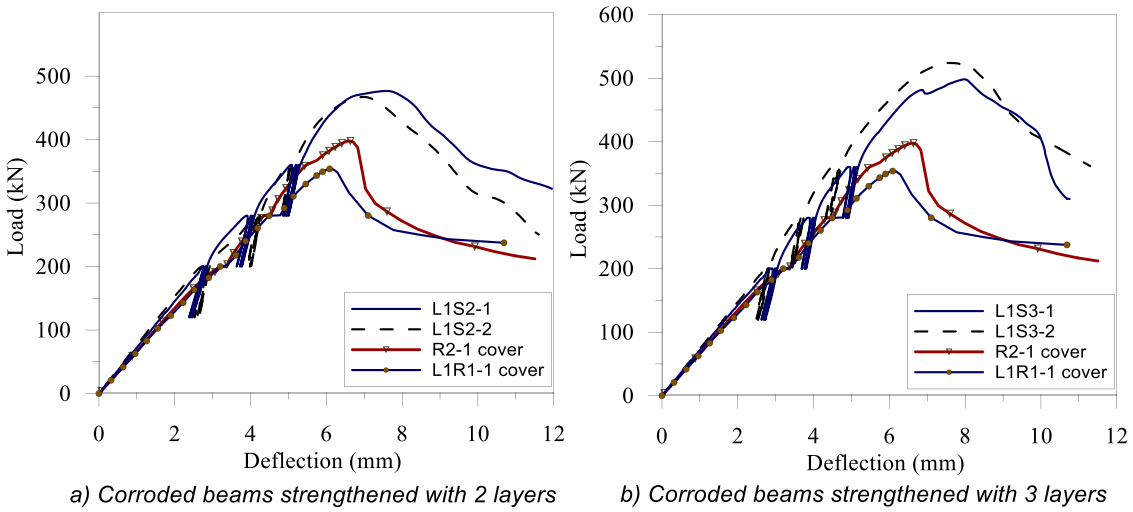

Fig. 16. Load-deflection of corroded-strengthened specimens in Group 2.

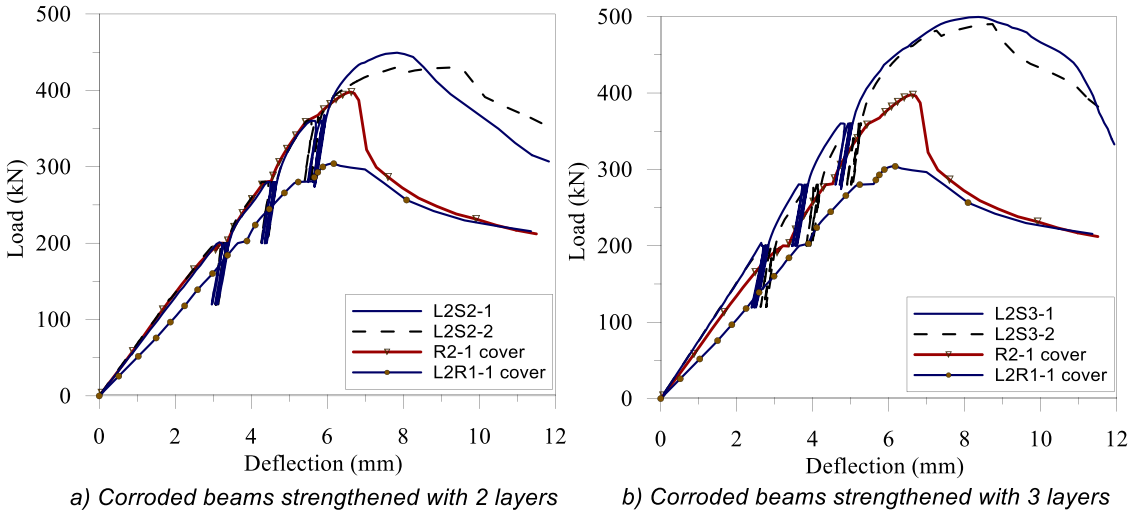

Fig. 17. Load-deflection of corroded-strengthened specimens in Group 3.

short-span corroded RC beams' overall performance in terms of ultimate load and stiffness. In contrast, the deflection at maximum load is similar for all specimens in this group. The specimens L2S2-1 and L2S2-2 also failed in shear due to textile rupture in the TRC layer, followed by inclined cracks' extension. However, the diagonal cracks in the beams strengthened with 2-layers-TRC were more distributed than those in the unstrengthened beams. This would increase the effectiveness of the TRC layer, and consequently, the shear force carrying capacity of the beams. These specimens reached the ultimate loads of 449.2 and 430.6 kN. The shear strength in the specimen strengthened by the 2-layer-TRC improved 42.5% compared to the controlled specimen, whereas the increment in the specimen repaired by the 3-layer-TRC is 60.6%. As expected, the stiffness of the strengthened beams increased with the number of layers of fabric, as indicated by the decrease in deflections. Failure in the TRC-strengthened layers started with crack propagation in the concrete matrix, and then textile rovings ruptured. It means that the interfacial bond between the TRC layer and the concrete substrate was efficient. In Group G3, the average degree of corrosion was 22.6%, much higher than those in Group G2 (12.7%).

The experimental results observed from 4 strengthened beams in Group 3 showed that the TRC strengthening layer helped to restore both strength and stiffness of the controlled-corroded beams. For the 3-layers strengthened beams, due to the high carbon textile reinforcement ratios, the failure mode changed from the critical shear cracks on the test side to the crushing failure on the strong side. It means that the tensile strength of carbon textiles could not be fully exploited.

5. Conclusions

The use of carbon TRC is an effective method for repairing and rehabilitating short-span corroded RC beams. Based on the

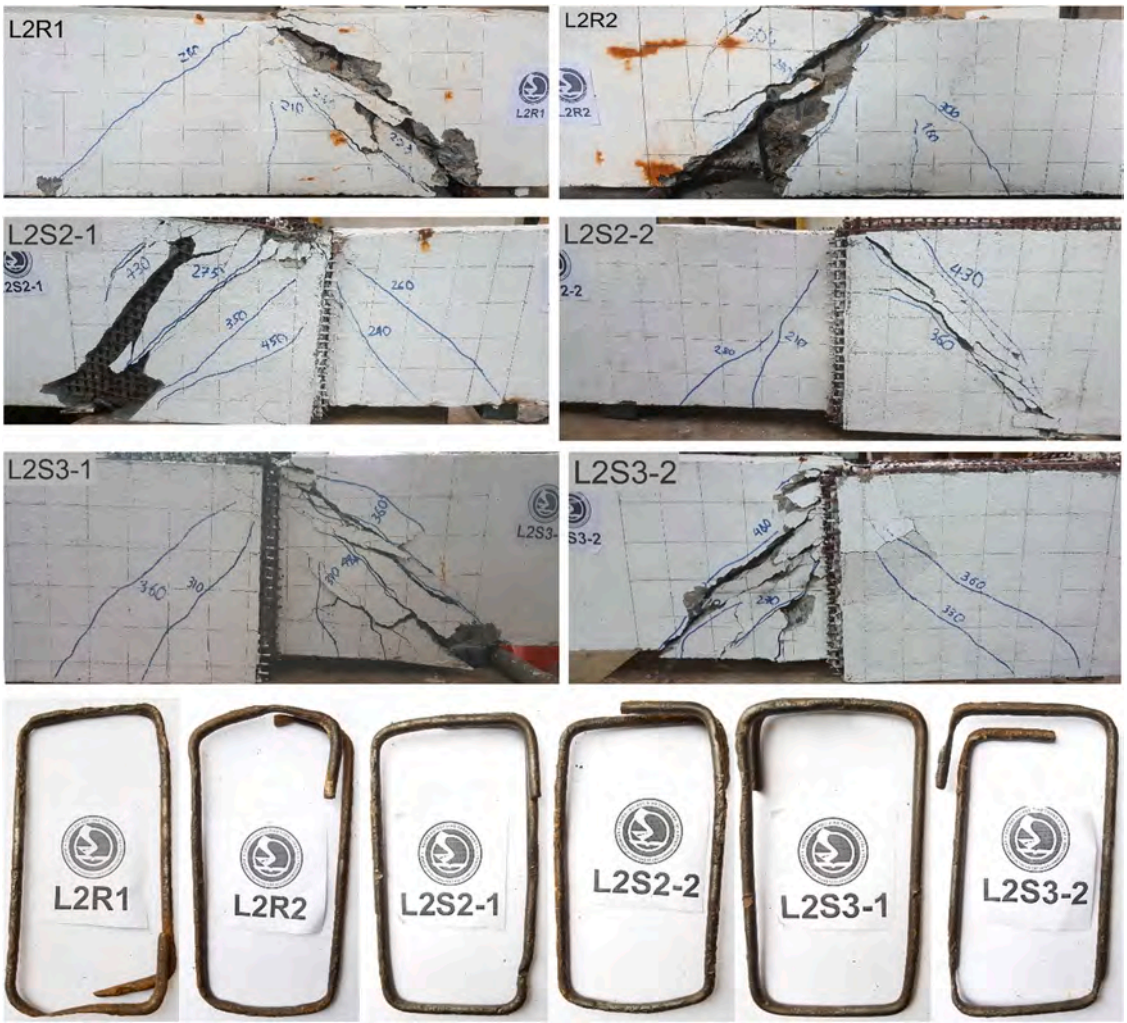

Fig. 18. Crack patterns of corroded beams in 3rd group and the extracted-corroded stirrups.

experiments performed in this study, conclusions are as follow:

- The shear capacity in the specimen reinforced with steel stirrups had been improved by 74.5% compared to the control beams without stirrups.
- The static-loaded and repeat-loaded RC beams have a similar performance in shear strength, failure mode, crack distribution, and load-deflection relationship. These beams failed in shear, with the shear cracks having a dominant development compared with flexural cracks for un-corroded specimens. However, the cracks of the repeat-loaded beams have grown in number and width than those of the static-loaded beams. The beams after repeated loading have residual deflections compared with the static beams.
- The loss of shear capacity of corroded RC beams increased as the corrosion rate increased. Compared to the controlled specimens, the averaged shear strength of corroded specimens decreased by 16.08% and 25.34%, corresponding to the degree of corrosion ranging from 12.3% to 23.6%.
- Reinforcement corrosion tends to reduce the stiffness of the reinforced concrete beam significantly at higher degrees of reinforcement corrosion. The stiffness of the corroded beams L1R1 and L1R2 (with a smaller degree of corrosion) was not much affected by corrosion despite the reduction in shear resistance.
- The experimental results showed that U-wrapping TRC strengthening methods helped enhance the corroded RC beams' stiffness, deformation, and strength. In the moderate corroded beams in Group G2, compared to the corroded-controlled specimens, the shear strength of strengthened specimens with 2 and 3 textile layers increased by 34.6% and 51.0%, respectively. For the severely damaged beams in Group G3, the shear strength in the specimen strengthened by the 2-layers and 3-layers had been improved 42.5% and 60.6% compared to the controlled specimens. Thus, the carbon TRC could restore and upgrade the damaged specimens to the original shear capacity of the uncorroded beams.

– The failure was attributed to the rupture of textile rovings in the U-wrapped layers, followed by the large inclined cracks at the "test side" of strengthened specimens with two-carbon layers. However, For the 3-layers-TRC strengthened beams, due to the high carbon textile reinforcement ratios, the failure mode changed from the critical shear cracks on the test side to the crushing failure on the strong side.

Declaration of Competing Interest

The authors declare that they have no known competing financial interests or personal relationships that could have appeared to influence the work reported in this paper.

Acknowledgments

The research is funded by the Vietnam Ministry of Education and Training under Grant no. CT2020.04.GHA.04.

References

[1] Y. Zhou, M. Guo, L. Sui, F. Xing, B. Hu, Z. Huang, Y. Yun, Shear strength components of adjustable hybrid bonded CFRP shear-strengthened RC beams, Compos. Part B: Eng. 163 (2019) 36–51.
[2] ACI Committee, ACI 549.4R-13: Guide to Design and Construction of Externally Bonded Fabric-Reinforced Cementitious Matrix (FRCM) Systems for Repair and Strengthening Concrete and Masonry Structures, American Concrete Institute, 2013.
[3] L. Koutas, Z. Tetta, D. Bournas, T. Triantafillou, Strengthening of concrete structures with textile reinforced mortars: state-of-the-art review, J. Compos. Constr. 23 (2019) 23.
[4] L. Wei, J.-H. Zhu, T. Ueda, M. Su, J. Liu, W. Liu, Tensile behaviour of carbon fabric reinforced cementitious matrix composites as both strengthening and anode materials, Compos. Struct. 234 (2019), 111675.
[5] A. Asgharzadeh, M. Raupach, Development of a Test Method for the Durability of Carbon Textiles Under Anodic Polarisation, Service Life and Durability of Reinforced Concrete Structures, Springer International Publishing, Cham, 2019.
[6] A. Brückner, R. Ortlepp, M. Curbach, Textile reinforced concrete for strengthening in bending and shear, Mater. Struct. 39 (8) (2006) 741–748.
[7] A..Wiberg, Strengthening of Concrete Beams Using Cementitious Carbon Fibre Composites (Doctoral thesis), Royal Institute of Technology, Stockholm, Sweden, 2003.
[8] S. Babaeidarabad, G. Loreto, A. Nanni, Flexural strengthening of RC beams with an externally bonded fabric-reinforced cementitious matrix, J. Compos. Constr. 18 (5) (2014), 04014009.
[9] A. D'Ambrisi, F. Focacci, Flexural strengthening of RC beams with cement-based composites, J. Compos. Constr. 15 (5) (2011) 707–720.
[10] M.E. Hussein, T.H. Almusallam, S.H. Alsayed, Y.A. Al-Salloum, Flexural strengthening of RC beams using textile reinforced mortar – experimental and numerical study, Compos. Struct. 97 (2013) 40–55 (March 2013).
[11] L.H. Sneed, S. Verre, C. Carloni, L. Ombres, Flexural behavior of RC beams strengthened with steel-FRCM composite, Eng. Struct. 127 (2016) 686–699.
[12] T.C. Triantafillou, C.G. Papanicolau, Shear strengthening of reinforced concrete members with textile reinforced mortar (TRM) jackets, Mater. Struct. 39 (1) (2006) 93–103.
[13] A. Brückner, R. Ortlepp, M. Curbach, Anchoring of shear strengthening for T-beams made of textile reinforced concrete (TRC), Mater. Struct. 41 (2) (2008) 407–418.
[14] T. Blänksvard, B. Täljsten, A. Carolin, Shear strengthening of concrete structures with the use of mineral based composites, J. Compos. Constr. 13 (1) (2009) 25–34.
[15] A. Si Larbi, R. Contamine, E. Ferrier, P. Hamelin, Shear strengthening of RC beams with textile reinforced concrete (TRC) plate, Constr. Build. Mater. 24 (10) (2010) 1928–1936.
[16] R. Contamine, A. Si Larbi, P. Hamelin, Identifying the contribution mechanisms of textile reinforced concrete (TRC) in the case of shear repairing damaged and reinforced concrete beams, Eng. Struct. 46 (2013) 447–458.
[17] C. Escrig, L. Gil, E. Bernat-Maso, F. Puigvert, Experimental and analytical study of reinforced concrete beams shear strengthened with different types of textile-reinforced mortar, Constr. Build. Mater. 83 (2015) 248–260.
[18] Z.C. Tetta, L.N. Koutas, D.A. Bournas, Textile-reinforced mortar (TRM) versus fiber-reinforced polymers (FRP) in shear strengthening of concrete beams, Compos. Part B: Eng. 77 (2015) 338–348.
[19] T.C. Triantafillou, C.G. Papanicolaou, Shear strengthening of RC members with textile reinforced mortar (TRM) jackets, Mater. Struct. RILEM 39 (1) (2006) 85–93.
[20] M. Elghazy, A. El Refai, U. Ebead, A. Nanni, Corrosion-damaged reinforced concrete beams repaired with fabric-reinforced cementitious matrix (FRCM), J. Compos. Constr. 22 (2018), 04018039.
[21] T. El-Maaddawy, A.E. Refai, Innovative repair of severely corroded T-beams using fabric-reinforced cementitious matrix, J. Compos. Constr. 20 (3) (2016), 04015073.
[22] L. Fang, Y. Zhou, D. Yi, W. Yi, Experimental study on flexural capacity of corroded RC slabs reinforced with basalt fiber textile, Appl. Sci. 11 (2020) 144.
[23] S. Oluwadahunsi, C.K.S. Moy, Performance of corroded reinforced-concrete beams in flexure strengthened using different basalt fiber textile-reinforced mortar schemes, J. Compos. Constr. 24 (6) (2020), 04020061.
[24] ACI Committee 434, (ACI434-2016) Acceptance criteria for masonry and concrete strengthening using fabric-reinforced cementitious matrix (FRCM) and steel reinforced grout (SRG) composite system, no. 800, 2017.
[25] RILEM Technical Committee 232-TDT, Recommendation of RILEM TC 232-TDT: test methods and design of textile reinforced concrete, 2016.
[26] Zulassung Z-31.10-182, Gegenstand: Verfahren zur Verstärkung von Stahlbeton mit TUDALIT (Textilbewehrter Beton), Prüfstelle: DIBt, Antragsteller: TUDAG TU Dresden Aktiengesellschaft, 2015.